Averaging effects of a strain gage [†]

N. T. Younis[*] and B. Kang

Department of Engineering, Indiana University - Purdue University Fort Wayne, 2101 E Coliseum Blvd, Fort Wayne, Indiana 46805, USA

Abstract

Choosing the right strain gage for a measurement application requires selecting gages with the right characteristics for the job. In general, the strain gage is to be used to measure the strain at the center of the gage, but it inherently underestimates the peak strain when it is mounted in high stress gradient areas. This paper concerns itself with the averaging effects of a strain gage along gage filaments. The approach is unconventional in dealing with the orientation and size of the gage. The results provide insight into the averaging effect and selecting gages for measuring strains in areas of steep strain gradients. Dimensionless curves which can be used to estimate errors as well as enhance hole-drilling method results are presented. Practical recommendations are made for selecting gages for high strain gradient measurements.

Keywords: Average strain; Experimental stress analysis; Strain gage; Stress concentration factor

---

1. Introduction

For members of complex shapes subjected to loads, it may be mathematically impractical or impossible to derive analytical load-stress relations. Thus, experimental or numerical methods are used to obtain results. An experimental analysis of component stresses is desired, either as an absolute determination of actual stresses or as validation for a numerical model that will be used for subsequent analysis. Several experimental methods are used, with the most common being the use of strain gages. The electrical resistance strain gage is the most frequently used device in stress analysis work. These gages are relatively inexpensive, reasonably durable, easy to mount on a surface, and are the most versatile means of measuring strain at a given point.

The strain gage is not meant to be used to measure strain other than at the center of the gage. Thus, error is introduced when the gage is used to measure strain at discontinuities such as holes, notches, and crack tips--areas of steep strain gradients. This error is due to the fact that the center strain underestimates the peak strain and is not an accurate representation of the stress field. In the field of fracture mechanics, some researchers use the gage reading as the strain at the center of the gage to determine the mode one stress intensity factor (K_I). Therefore, the literature is inconclusive regarding the location,

size, and orientation of the gage. For example, Dally and Sanford developed a method that utilizes strain gages for determining K_I [1]. An overdeterministic approach was developed for measuring K_I using data from three 10-element strip strain gages with some accuracy [2]. The error generated in K_I due to placement errors in positioning and orienting the single gage was determined [3, 4]. It was concluded that the deviation in the orientation angle of the strain gage is the dominant source of the error. A technique for determining the stress intensity factor using strain gages was developed in which the location of the strain gage relative to the crack tip was chosen through parametric study of the asymptotic fields [5]. In 2010, Sarangi et al. [6] proposed a finite element based method for determining the limiting radial distance of placing the strain gage in the vicinity of a crack tip.

Recently, the effect of strain gradient was mentioned or ignored by researchers in the field. To assure accuracy of determining structural gage sensitivity, Zhang et al. chose locations for the strain gage rosettes with a small strain gradient [7]. The hole-drilling method is the most common technique for measuring residual stresses in various materials and structures [8]. It utilizes strain gages around a circular hole. The practical disadvantage of this is that the strains measured are average values in the range of the length of the strain gage [9]. The correction of errors introduced by hole eccentricity has been proposed by Barsanescu and Carlescu [10]. In 2009, the performance of three dimensional strain gages embedded into a sphere was evaluated [11]. In the case of a high strain gradient, the calculated strain tensor is subject to errors and this prob-

lem can be overcome by embedding the gages in a sphere at a specified orientation relative to the center of the sphere.

The subject of error in a strain measurement system using a metal-foil sensing grid is complex, as documented by many researchers in the field. For example, Pople listed the human factor errors and error sources in strain gage measurement [12]. Perry presented an extensive report that examined several fundamental properties of the strain gage that are involved in measurement accuracy [13]. These properties are the gage factor, reinforcement effects, transverse sensitivity, thermal effects, and area averaging effect of a square gage. The theoretical errors caused by thermal effects and gage factor data given by the manufacturers were studied by Cappa [14]. Zubin [15] carried out a theoretical error investigation of calibration beams used for the determination of the gage factor. In 2005, a computer simulation of strain gage thermal effect errors during residual stress hole drilling measurements was carried out and is presented in reference [16]. In 2006, Robinson discussed the fact that stress analysis engineers are probably no more aware of the background regarding some aspects of the gages than is the average person [17].

In the present study, a detailed analysis of the strain averaging characteristic of the strain gage is presented. For more accurate error analysis, the averaging approach is over the resistive filaments since they cover only a portion of the gage's area. A classical plate with a circular hole subjected to uniaxial loading is used as a vehicle for examining the effects of misalignment, length, width, and number of filaments on the average strain experienced by the gage. The analysis shows that the output of the strain gage is influenced by the number of filaments.

2. Theory

The strain gage is a type of electrical resistor. Most commonly, strain gages are thin metal-foil grids that are bonded to the surface of a machine part or a structural member. When forces are applied to the member, the gage elongates or contracts with the member, creating normal strains. The change in length of the gage alters its electrical resistance. By measuring the unbalanced voltage in Wheatstone bridge due to the change of electrical resistance of the wire, the gage can be calibrated to directly read values of normal strain.

Since the gage is of finite length, the change in resistance is due to the average strain along the gage and not the center strain in general. If the strain along the gage is constant or linear, the average strain is the same as that of the center strain. However, for a stress concentration problem, the average strain will differ from the center strain. When the strain gradient is large, the average strain is lower than the true strain at a given point. Therefore, the indicated strain will be in error of the true strain. The thin plastic backing is an integral part of basic gage construction. However, conformance to measure peak strain in the vicinity of stress concentration will be reduced.

Each gage consists of a fine metal grid that is stretched or shortened when the object is strained at the area where the gage is attached. The grid is equivalent to a continuous wire that goes back and forth from one end of the grid to the other, therefore effectively increasing its length. The grid of bonded foil gage, shown in Fig. 1(a), is the major source of error introduced by the strain gage when it is used to measure strain at the edge of the hole. The electrical resistance strain gage measures the average strain of each filament and the indicated strain is the average of the filaments strains. Using the points shown in Fig. 1 (a), the indicated strain is:

$$\varepsilon_{\text{indicated}} = \frac{\varepsilon_{AB} + \varepsilon_{CD} + \varepsilon_{EF} + \varepsilon_{GH}}{\text{number of filaments}} \ . \tag{1}$$

One of the most important problems in the design of plate structures is to determine the stress concentration due to the presence of holes and other discontinuities. The approach can be extended to other discontinuities by changing the stress field equations. The classical Kirsch [18] solution for the stresses around a circular hole in a large plate with normal stress σ_0 applied at infinity in the *Y*-direction, as shown in Fig. 1(a), is given by:

$$\sigma_{rr} = \frac{\sigma_0}{2}\left[\left(1 - \frac{a^2}{r^2}\right)\left(1 + \left(3\frac{a^2}{r^2} - 1\right)\cos 2\theta\right)\right] \tag{2a}$$

$$\sigma_{\theta\theta} = \frac{\sigma_0}{2}\left[\left(1 + \frac{a^2}{r^2}\right) + \left(1 + 3\frac{a^4}{r^4}\right)\cos 2\theta\right] \tag{2b}$$

$$\tau_{r\theta} = \frac{\sigma_0}{2}\left[\left(1 + 3\frac{a^2}{r^2}\right)\left(1 - \frac{a^2}{r^2}\right)\sin 2\theta\right] \tag{2c}$$
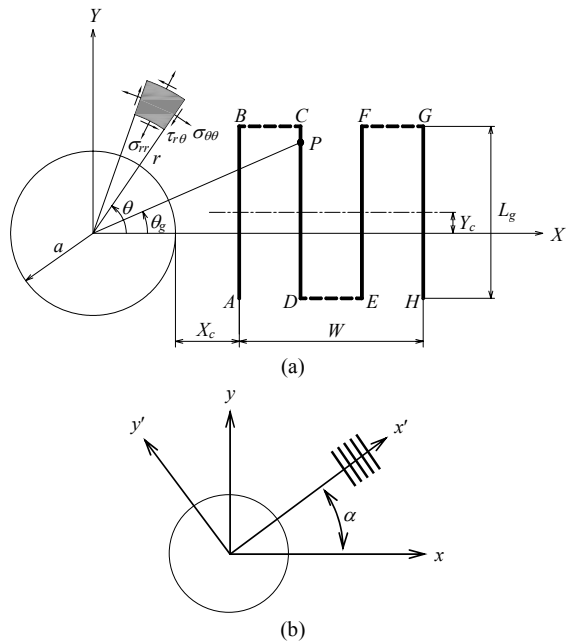

Fig. 1. Definition of the strain gage geometry.

In the end, the strain averaging of the gage is computed by integrating the strains along the gage filaments, for which the strain in the *Y*-direction is needed along each filament. This requires converting the stresses in the *r-θ* coordinate system to ones in the *X-Y* coordinate system. Upon applying the standard stress transformation equations, the stresses at point *P* can be found by:

$$\sigma_X = \sigma_{rr}\cos^2\theta_g + \sigma_{\theta\theta}\sin^2\theta_g + 2\tau_{r\theta}\cos\theta_g\sin\theta_g \quad (3a)$$

$$\sigma_Y = \sigma_{rr}\sin^2\theta_g + \sigma_{\theta\theta}\cos^2\theta_g + 2\tau_{r\theta}\cos\theta_g\sin\theta_g \quad (3b)$$

or, due to $r^2 = X^2 + Y^2$ and $\theta_g = \tan^{-1}(Y/X)$,

$$\sigma_x = \frac{\sigma_0}{2}\left[\frac{1}{r^2}\left(1-\frac{3}{r^2}\right)+\frac{6}{r^4}\left(\frac{2}{r^2}-1\right)x^2 \right. $$
$$\left. +\frac{4}{r^6}\left(2-\frac{3}{r^2}\right)x^4+\frac{4}{r^6}\left(\frac{3}{r^2}-2\right)x^2y^2\right] \quad (4a)$$

$$\sigma_y = \frac{\sigma_0}{2}\left[2-\frac{1}{r^2}\left(1-\frac{3}{r^2}\right)+\frac{2}{r^4}\left(1-\frac{6}{r^2}\right)x^2 \right.$$
$$\left. -\frac{4}{r^4}y^2+\frac{12}{r^8}x^4+\frac{4}{r^6}\left(4-\frac{3}{r^2}\right)x^2y^2\right] \quad (4b)$$

$$\tau_{xy} = \frac{\sigma_0}{2}\left[\frac{1}{r^4}\left(\frac{12}{r^2}-10\right)xy+\frac{1}{r^6}\left(16-\frac{24}{r^2}\right)x^3y\right] \quad (4c)$$

Note that the *X* and *Y*-coordinates have been normalized against the hole's radius; i.e., $x = X/a$, $y = Y/a$, and $\bar{r}^2 = x^2 + y^2$. The distribution of σ_x/σ_0 is plotted as a function of position along the *x*-axis for various values of *y* in Fig. 2(a). An exami-
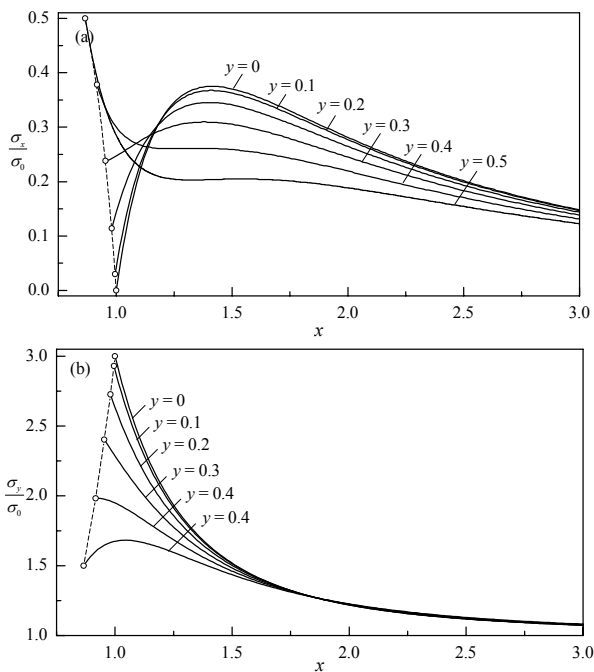
nation of this figure clearly indicates that the transverse stress is zero at the edge of the hole (*x*=1) and varies in different patterns as *y* increases from 0 to 0.5. Thus, there is no area to mount the gage on that will represent the average σ_x. A perfect gage installation would be at *x*=1 when the gage filaments are perpendicular to the *x*-axis. To account for the expertise of the user (tilting the gage), the distributions at *x* less than 1 are plotted. With the hole center at the origin, the variation of σ_y/σ_0 of Eq. (4b) in the *x* direction at *y*=0, 0.1, 0.2, 0.3, 0.4, and 0.5 is plotted in Fig. 2(b). Examining the stress curves, one can see that the slopes change not only in magnitude, but also in sign, from negative to positive and vice versa.

Stress is a mathematical abstraction, and it cannot be measured. Strains, on the other hand, can be measured directly through well-established experimental procedures such as strain gages. Once the strains in a component have been measured, the corresponding stresses can be calculated using stress-strain relationships such as the generalized Hook's law. However, in this study, the strains need to be calculated utilizing stress equations. The stress-strain relations for a two-dimensional state of stress are:

$$\varepsilon_x = \frac{1}{E}\left(\sigma_x - \nu\sigma_y\right) \quad \varepsilon_y = \frac{1}{E}\left(\sigma_y - \nu\sigma_x\right) \quad (5a)$$

$$\gamma_{xy} = \frac{\tau_{xy}}{G} = 2(1+\nu)\frac{\tau_{xy}}{E} \quad (5b)$$

Shown in Fig. 3 is the distribution of σ_y in the first quadrant of the *x-y* plane for $\sigma_x/E=1$ and $\nu=0.3$. It can be seen that the maximum value is 3 at *x*=1 and *y*=0, which is well known as the maximum stress concentration factor σ_y/σ_0 for the present case. Note also that, although not clearly shown in the graph, $\varepsilon_y = \nu$ at *x*=1 and *y*=0 since $\sigma_x/\sigma_0 = -1$ and $\sigma_y = 0$ at that point. The results show that the average strain does not equal the strain at the gage center.

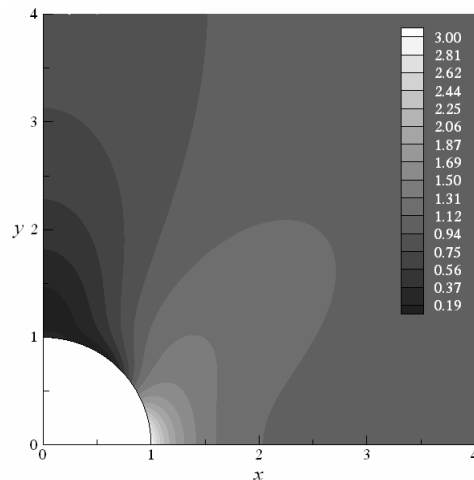The gage filament covers only a portion of its area as shown

Fig. 2. Distribution of (a) σ_x/σ_0 and (b) σ_y/σ_0 along the *x*-axis around the hole's boundary for ν=0.3.

Fig. 3. ε_y in the first quadrant of the *x-y* plane for $\sigma_0/E=1$ ν=0.3.

in Fig. 1(a). This fact needs to be accounted for in the analysis of errors due to strain gage placement. The strain averaging of the gage is modeled by integrating the strains along the filaments placed near the hole. Consider a strain gage placed near the hole edge as shown in Fig. 1(a). For computational purposes, it is advantageous to compare the size and location of the gage to the hole radius a, hence the gage parameters are normalized against the radius of the hole. It is assumed that the edge of the gage (or the first filament) is at distance $x_c = X_c/a$ from the edge of the hole, and the vertical center of the gage is displaced from the lateral axis of the hole by $y_c = Y_c/a$. The width of the gage is $w = W/a$ and the length is $l_g = L_g/a$. It is also assumed that the filaments are evenly spaced across the width. Then, the average strain experienced by a strain gage with n filaments placed in the y-direction can be determined from

$$\varepsilon_{avg} = \frac{1}{nl_g} \sum_{k=1}^{n} \int_{y_c - l_g/2}^{y_c + l_g/2} \varepsilon_{yk} \, dy \tag{6}$$

where the ε_{yk} denotes the strain in the kth filament that can be found by

$$\varepsilon_{yk}(x,y) = \begin{cases} \varepsilon_y(1 + x_c, y) & \text{for } n = 1 \\ \varepsilon_y\left(1 + x_c + \dfrac{(k-1)w}{n-1}, y\right) & \text{for } n \geq 2 \\ & \text{and } (k = 1, 2, \cdots, \leq n) \end{cases} \tag{7}$$

The integral in Eq. (6) can be readily evaluated using various numerical integration algorithms. In addition, it can be noticed that the continuous average strain $\bar{\varepsilon}_{avg}$ (i.e., the average strain taken over the gage's grid area) corresponds to the average strain when $n=\infty$; i.e.,

$$\bar{\varepsilon}_{avg} = \lim_{n \to \infty} \varepsilon_{avg} = \frac{1}{l_g w} \int_{y_c - l_g/2}^{y_c + l_g/2} \int_{1+x_x}^{1+x_c+w} \varepsilon_y(x,y) \, dx \, dy \tag{8}$$

Note that the above $\bar{\varepsilon}_{avg}$ is equivalent to the average strain used by Perry [13] to address the averaging effect of strain gage size.

Another important factor that accounts for a significant measurement error of strain gage is the angular misalignment of the strain gage. For a strain gage misaligned by an angle α as shown in Fig. 1(b), the actual reading of normal strains in the x' and y' directions can be found by transforming the strains defined in the x and y coordinates according to

$$\varepsilon_{x'} = \varepsilon_x \cos^2 \alpha + \varepsilon_y \sin^2 \alpha + \gamma_{xy} \cos \alpha \sin \alpha \tag{9a}$$

$$\varepsilon_{y'} = \varepsilon_x \sin^2 \alpha + \varepsilon_y \cos^2 \alpha - \gamma_{xy} \cos \alpha \sin \alpha \tag{9b}$$

The average strain experienced by a strain gage with n filaments placed in the y'-direction can be found from

$$\varepsilon_{avg} = \frac{1}{nl_g} \sum_{k=1}^{n} \int_{y_c - l_g/2}^{y_c + l_g/2} \varepsilon_{y'k} \, dy \tag{10}$$

The average strain becomes a function of six variables: i.e.,

$$\varepsilon_{avg} = f(w, l_g, x_c, y_c, \alpha, n) \tag{11}$$

3. Results and discussion

It is assumed that no shear lag occurs across the adhesive line, thus the strain felt by each gage filament is the same as the strain in the plate directly below it. The strain is averaged over each filament length. The gages consist of a grid of very fine wire or foil. Therefore, it is assumed that the strain does not vary across an individual filament and the strains at the midline of the filaments are used in the averaging process. The filaments are evenly spaced across the width. There are at least 8 filaments in a general purpose strain gages-linear pattern. Although the case in which $n=1$ or 2 is for semiconductor gages, it is considered here in order to examine the results of reducing the number of resistive filaments.

In stress analysis applications, it is important to examine potential error sources prior to taking data. Eqs. (6) - (10) provide a theoretical framework for evaluating the influences of each of the 6 parameters considered in this study. Several examples are presented to illustrate the magnitudes of error that are possible. The percent error e is defined with respect to the actual strain to be measured (ε_{act}) at $x=1$ and $y=0$ such that $e = (1 - \varepsilon_{avg}/\varepsilon_{act}) \times 100$ [%] and is used for the following case studies. Note that ε_{act} is the same as the maximum normal strain for the plate considered in these examples.

Case 1: In the first case the gage length is held constant while the gage width is varied. Both x_c and y_c are zero. The error analysis is very conservative because the matrix width is greater than the grid width. Active grid length does not include end loops or tabs. Fig. 4 shows the variation of the averaging strain with w for different numbers of filaments. Additional filaments further away from the hole increase the error for a given width gage. A single filament at the hole's edge gives an error of 7.24%. It is important to note that these error curves are for the same model, i.e. the same hole, material,
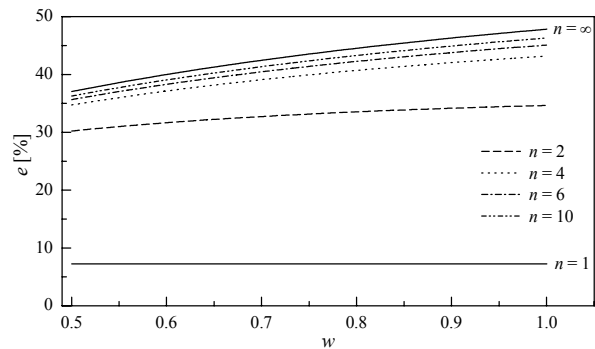

Fig. 4. Effect of gage's width ($w=W/a$) on error for $l_g=0.5$ and $x_c=y_c=0$.

and applied load, yet the strain is a function of the gage width and the number of filaments. For w=0.5, the difference in errors between n=2 and n=10 is 6% while the difference in errors between n=2 and n=10 for w=1 is 11.7%. One can conclude that the spacing between the filaments of a strain gage contributes to the error in measuring the strain. However, as an example for n=2, the difference in errors between w=0.5 and w=1 is 4.4%. Thus, the number of filaments is the dominant factor in the assessment of the error in strain gage measurements at regions of stress concentration. As a rule of thumb, the gage size should be very small compared to the hole size. However, small strain gages tend to exhibit degraded performance in terms of the maximum allowable elongation, the stability under static strain, and the endurance when subjected to alternating cyclic strain [8].

Case 2: In this case, the gage width is kept constant (w=0.5) and the gage length l_g is varied. Larger gages are more resistant to localized temperature and strain effects and are easier to handle due to their larger size. The minimum percent error versus the gage length for different numbers of filaments is shown in Fig. 5. It is clear that the average strain is a function of the gage length including the gage with a single filament. However, for a given load, the strain at the edge of the hole is constant. The difference in errors between a single filament and two filaments is large for the same l_g. The results show that the difference in errors between n=2 and n=10 is 6% for l_g=0.5, however it is 7% between l_g=0.5 and l_g=1 for n=2. Therefore, both gage length and the number of filaments should be considered in the assessment of the error of the average strain in regions of high strain gradient. The user can select the smallest practicable gage length, but needs to be aware of the greatly increased error and uncertainty in the indicated strains due to the nature of the gage and instrumentations. It is worth noting that using relatively large strain gages enhance the accuracy of measuring strain at a high strain gradient [19].

Case 3: In this case, both the gage length (l_g=0.5) and width (w=0.5) are held constant while the horizontal distance from the hole's edge to the first filament is varied. This is due to the inherent gage manufacturing process and human-dependant error source. The metal-foil strain gage is the most frequently employed gage for both general-purpose stress analysis and transducer applications. The grids are very fragile and easy to distort, wrinkle, or tear. For this reason, foil gages are generally mounted on a thin epoxy carrier or paper or sandwiched (encapsulated) between two thin sheets of epoxy; this improves the temperature range, fatigue life, and chemical mechanical protection of the sensing grid. The dimensions of the matrix (sheets) are larger than that of the sensing grid. Hence, obtaining x_c=0 in engineering practice is very difficult. The results are shown in Fig. 6. The difference in errors between n=2 and n=10 for x_c=0 is 6%. However, for n=2, the difference in errors between x_c=0 and x_c=0.5 is 27.4%. This clearly shows that the predominant factor in the error of the average strain is the inherent lateral gap of the gage. The results sug-
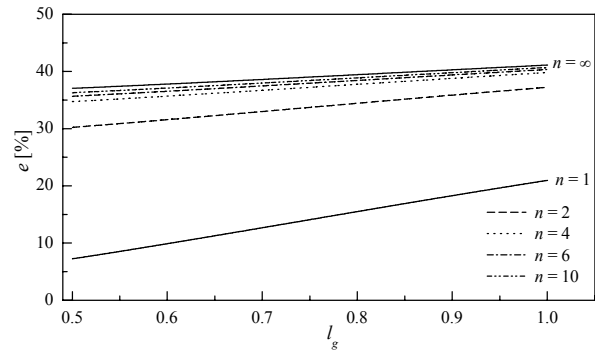

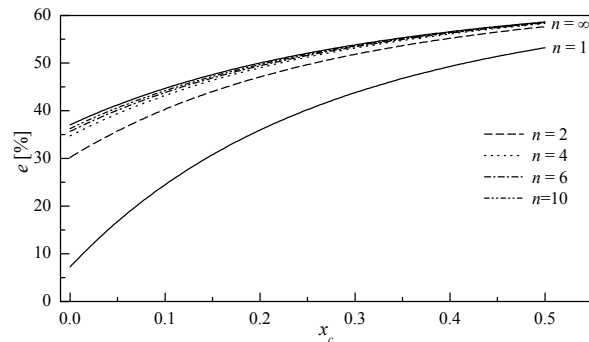Fig. 5. Effect of gage's length (l_g=L_g/a) on error for w=0.5 and x_c=y_c=0.

Fig. 6. Effect of gage's lateral misalignment (x_c=X_c/a) on error for w=0.5 and l_g= 0.5.

gest the manufacturing of special use strain gages – stress gradient. The results also indicate that the number of filaments contributes significantly to the error of the strain measured at a stress concentration area.

Case 4: This case deals with the misplacement of the strain gage, which is a typical human-dependant error. The distance between the hole's x-axis and the gage's horizontal center line is y_c. The carrier dimensions are designed for the optimum function of the strain gage and are larger than the sensing filaments. Thus, obtaining y_c=0 in most practical situations is very difficult even for an experienced operator with considerable skill and agility. Fig. 7 shows the strain averaging effect versus y_c for w=l_g=0.5. The results show that the number of filaments and gage mispositioning contribute to the error of the average strain. For example, the percent difference of the average strain between n=2 and n=10 for perfect gage alignment (y_c=0) is 6%. The difference of the average strain between a properly aligned gage and a gage displaced from the x-axis of the hole by y_c=0.3 is 9.5% for n=2. Another common human-dependent error in strain measurement is the angular misalignment of the gage, as depicted in Fig. 1(b). It is examined by varying the tilt angle α measured with respect to the x-axis of the hole while holding x_c=0.05 and y_c=0. Results from Eq. (10), illustrated for α=0-20° in Fig. 8, indicate that the angular misalignment of the strain gage is another substantial source of strain measurement error.

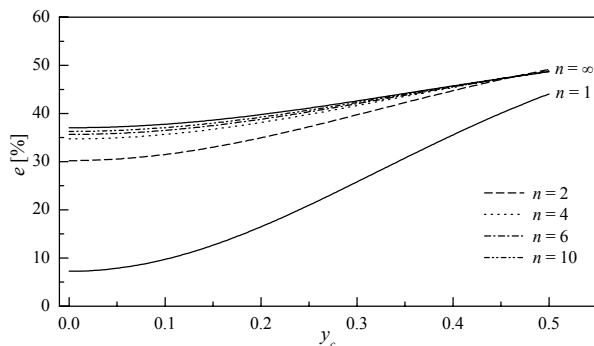From the results obtained, the error of measuring the strain

Fig. 7. Effect of gage's vertical misalignment ($y_c=Y_c/a$) on error for w=0.5 and l_g=0.5.
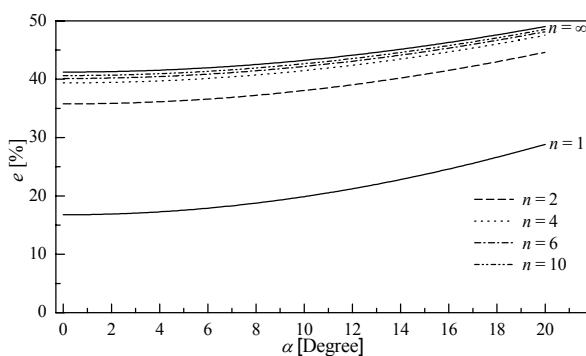

Fig. 8. Effect of gage's angular misalignment (α) on error for x_c=0.05, y_c=0, w=0.5, and l_g= 0.5.

at the edge of a hole using strain gages can be clearly shown in Figs. 4-8. Each curve on the graphs represents the strain experienced by the gage for a given number of filaments. As the number of filaments changes, the strain also changes. The strain in the vicinity of a hole is constant under a fixed applied load, but the strain gage results depend on the number of filaments. This shows that there is an error in the strain gage measurement and that the number of filaments has a large influence on the average strain near an area of stress concentration. Therefore, the strain at the center of the gage underestimates the actual strain.

4. Summary and Conclusions

To select the proper stain gage, pattern and size, the averaging effect error of the gage is analyzed. Four cases were investigated for which the error magnitudes cannot be adequately compensated by even a competent stress analyst. In each case, the effects of the number of filaments on the average strain were studied. Case 1 involved the effect of the gage width and Case 2 examined the effect of the gage length. Cases 3 and 4 investigated the mispositioning and orientation of the strain gage. The results of these case studies are summarized in Figs. 4-8. It is believed that these results can provide insight to the behavior of the averaging effect of the strain gage. In the case of other high strain gradients, the results reported here cannot be quantitatively precise. However, it is practical that the error

magnitudes may be used as an estimate to correct the readings of gages in unknown strain fields. The theory can be extended to other discontinuities by changing the stress field equations. In addition, the results can be used to enhance the accuracy of the hole-drilling method.

Finally, the average strain over the gage filaments is not the same as the average strain over the gage grid area. It is concluded that the number of filaments plays an equally important role on the averaging effect as the gage dimension and orientation. Therefore, in order to reduce the averaging effect error, mounting a gage with very few filaments (custom stress gradient gage) would be recommended.

Nomenclature――――――――――――――――――

a	:	Radius of hole
x, y	:	Non-dimensional x-, y-coordinate, $x=X/a$, $y=Y/a$
$\sigma_{rr}, \sigma_{\theta\theta}, \tau_{r\theta}$	:	Plane polar stress components
$\sigma_x, \sigma_y, \tau_{xy}$	:	Plane Cartesian stress components
σ_0	:	Applied stress
$\varepsilon_x, \varepsilon_y, \gamma_{xy}$	:	Plane Cartesian stress components
$\varepsilon_{avg}, \overline{\varepsilon}_{avg}$	:	Average strains computed by Eq. (6) and Eq. (8)
ε_{act}	:	Actual strain
E, G	:	Young's modulus, Shear modulus, $G=E/2\,(1+\nu)$
ν	:	Poisson's ratio
n	:	Number of filaments of strain gage
l_g	:	Non-dimensional length of strain gage, $l_g=L_g/a$
w	:	Non-dimensional width of strain gage, $w=W/a$
x_c, y_c	:	Location of strain gage, see Fig. 1, $x_c=X_c/a$, $y_c=Y_c/a$
α	:	Tilt angle

References

[1] J. W. Dally and R. J. Sanford, Strain-gage methods for measuring the opening-mode stress-intensity factor, K_I, *Experimental Mechanics*, 27 (1987) 381-388.

[2] J. R. Berger and J. W. Dally, An overdeterministic approach for measuring K_I using strain gages, *Experimental Mechanics*, 28 (1988) 142-145.

[3] J. R. Berger and J. W. Dally, An error analysis for a single strain-gage determination of the stress-intensity factor K_I, *Experimental Techniques*, 12 (1988) 31-33.

[4] N. T. Younis and J. Mize, Discrete averaging effects of a strain gage at a crack tip, *Engineering Fracture Mechanics*, 55 (1996) 147-153.

[5] P. R. Marur and H. V. Tippur, A strain gage method for determination of fracture parameters in bimaterial systems, *Engineering Fracture Mechanics*, 64 (1999) 87-104.

[6] H. Sarangi, K. S. Murthy, and D. Chakraborty, Radial locations of strain gages for accurate measurement of mode I stress intensity factor, *Materials & Design*, in press.

[7] S. Y. Zhang, G. Prater, Jr., A. M. Shahhosseini and G. M.

Osborne, Experimental validation of structural gage sensitivity indices for vehicle body structure optimization, *Experimental Techniques*, 32 (2008) 51-54.

[8] *Strain Gage Selection, Criteria, Procedures, Recommendations*. Tech. Note TN-505-3, Measurements Group, Inc., Raleigh, North Carolina, USA.

[9] J. Chen, Y. Peng and S. Zhao, Comparison between grating rosette and strain gage rosette in hole-drilling combined systems, *Optics and Lasers in Engineering* 47 (2009) 935-940.

[10] P. Barsanescu and P. Carlescu, Correction of errors introduced by hole eccentricity in residual stress measurement by the hole-drilling strain-gage method, *Measurement*, 42 (2009) 474-477.

[11] P. Trench, E. G. Little, D. Tocher, P. O'Donnell and V. Lawlor, The performance of three-dimensional strain rosettes evaluated when embedded into a sphere, *Strain*, 45 (2009) 149-159.

[12] J. Pople, Error in strain measurement-the human factor (or how much do I contribute?), *Experimental Techniques*, 8 (1984) 34-38.

[13] C. C. Perry, The resistance strain gage revisited, *Experimental Mechanics*, 24 (1984) 286-299.

[14] P. Cappa, Random errors caused by temperature in magnitude of principal strains evaluated with 3-element strain gauge rosettes, *Strain*, 25 (1989) 139-144.

[15] D. Zubin, Theoretical design of calibration beams for strain gauge factor measuring apparatus, *Strain*, 34 (1998) 99-107.

[16] P. Litos, M. Svantner and M. Honner, Simulation of strain gauge thermal effects during residual stress hole drilling measurements, *The Journal of Strain Analysis for Engineering Design*, 40 (2005) 611-619.

[17] M. Robinson, Strain Gage Materials Processing, Metallurgy, and Manufacture, *Experimental Techniques*, 30 (2006) 42-46.

[18] J. W. Dally and W. F. Riley, *Experimental stress analysis*, McGraw-Hill, New York, USA (1991).

[19] S. Swamy, M. V. Srikanth, K. S. R. K. Murthy and P. S. Robi, Determination of mode I stress intensity factors of complex configurations using strain gages, *Journal of Mechanics of Materials and Structures,* 3 (2008) 1239-1255.

N. T. Younis received his Ph.D. degree from Iowa State University, USA, in 1988. He is currently a Professor of Mechanical Engineering at Indiana University – Purdue University Fort Wayne (IPFW). His research interests include solid mechanics, experimental stress analysis, and experimental fracture mechanics.